Synthesis of 2-hydroxynicotinaldehyde grafted isonicotinic acid hydrazide compounds and their antimicrobial evaluation

Lin Zhang, Hao Li, Fang Yang, Xiaoling Lu, Qi Yin,
Kang Yang, Zeng Yang, You Long, Chao Shen,
Bo Yao, Chenghong Huang [a, *]

School of Chemistry and Chemical Engineering, CQUST, Chongqing, China

[a] 2013008@cqust.edu.cn

Abstract. Bacterial infection is one of the main causes of disease and death, and most drugs show resistance during treatment. It is necessary to develop novel, efficient, and less toxic drugs to handle drug resistance. This study synthesized isoniazid/2-hydroxy nicotinoid Schiff base compounds using isoniazid and 2-hydroxy nicotinoid compounds as raw materials in a 40℃ water bath and further evaluated their antibacterial properties. The structure of isoniazid/2-hydroxynicotinal Schiff base compound was confirmed by FT-IR, 1H NMR, DSC, XRD and XPS. MIC against S.aureus and E.coli was determined by liquid method and plate method. The results showed that the new infrared absorption peak of isoniazid/2-hydroxynicotinal Schiff base compound at 1662cm-1 was formed by ligand imine group ν (C=N), and the melting peak decreased to 159℃. There was also a new diffraction peak at 2θ=10.74° on XRD spectra and chemical shift signal peak on 1H NMR spectrum. The characteristic peaks of XPS shift towards higher fields. MIC of isoniazid, 2-hydroxynicotinoid, and isoniazid/2-hydroxynicotinoid compounds against S.aureus and E.coli are 402.50μg/mL, 402.50μg/mL, 201.25μg/mL, and 402.50μg/mL, 402.50μg/mL, and 100.63μg /mL, respectively. SEM images reveal that isoniazid/2-hydroxynicotinoid compounds kill bacteria by disrupting cell membranes, and have better antibacterial effects compared to raw materials.

Keywords: isoniazid; 2-hydroxynicotinic aldehyde; Schiff base; antibacterial.

1. Introduction

Bacteria in environment can reside in animals and human body, and majority host-parasite relationships are harmful to human beings [1], and this parasitism can cause a variety of diseases and increase the morbidity and lethality of the hosts [2]. Common diseases caused by bacteria include upper respiratory tract infections, surgical wound infections, acute otitis media, sinusitis, skin and soft-tissue infections, intestinal mucosal infections, and endocarditis [3]. So sterilization is very important to promote public health. The two most common types of sterilization are chemical and physical methods. Physical sterilization is the process of killing microorganisms by using high temperatures, drying, radiation, sound waves, and other physical methods. Some of the techniques used to achieve this include microwave technology, red/ultraviolet irradiation, ionizing radiation, dry/moist heat sterilization, photothermal therapy, and photodynamic therapy, etc. [4]. Chemical sterilization refers to the use of chemicals that act directly on microorganisms to kill them, commonly used chemical drugs include nanase [5], ampicillin [6], amoxicillin [7], cefuroxime [8], vancomycin [9], milocycline [10], and moxifloxacin [11], etc. But in the same period of time, bacteria show various forms of resistance as prolonged or uncontrolled us of antibiotics[12]. resulting in resistance mechanisms become more complex. Emergence of multi-resistant superbugs [13] has posed a serious threat to public health. Therefore, development of new, efficient antibacterial drugs with bacteriostatic activity are urgent.

Isoniazid (4-pyridinecarbohydrazide,INH) is a derivative synthesized from nicotinic acid. INH is used as a first-line antituberculosis drug [14]. INH and its derivatives have excellent properties such as antituberculosis [15], antimicrobial [16], urease inhibitory activity [17], antidepressant [18] and analgesic [19]. It has been shown that heterocyclic-containing isonicotinoylhydrazone derivatives

had been demonstrated to have better antimicrobial activity [20], and in order to further extend the antimicrobial effect of INH and to reduce the cytotoxicity exhibiting in the therapeutic process, thus preparation of INH Schiff base derivatives has become a hot spot of research. Schiff bases (also known as imines) are compounds containing an imine or methyleneimine group (C=N) and often formed by the dehydration condensation of a primary amine group of one molecule with a carbonyl group of another molecule [21]. Schiff bases are a class of pharmacophore with multiple functions and its derivatives have excellent properties such as bacteriostatic [22], antiviral [23], anticancer [24], which are widely applied in the field of pharmaceuticals, materials, catalytic reagents, pesticides and biologically active reagents [25].Yasser et al [26] synthesized a new chitosan derivative(CHQ) by the reaction of chitosan with 2-chloro-3-formyl-7-ethoxyquinoline derivative. CHQ possesses excellent antimicrobial, antioxidantand antidiabetic properties, with maximum inhibition of 96% against Staphylococcus haemolyticus but 77% against E.coli. Yosef ect [27] synthesized three Schiff bases by the condensation of salicylaldehyde with 4-aminoantipyrine, ethylenediamine, and 2-aminophenol(L1, L2, L3) and in vitro antimicrobial activity was determined against two gram-positive (S.aureus, Staphylococcus epidermidis) and two gram-negative bacteria (Klebsiella pneumoniae and Pseudomonas aeruginosa), which showed that all three Schiff bases possess antimicrobial activity but only compound L3 was more active than the standard antibiotics, Ciprofloxacin and Chloramphenicol, against the bacteria. Emad et al [28] next synthesized 2-N-salicylaldehyde-5-(p-nitrophenyl)-1,3,4thiadiazole and [Vo(II), Co(II), Rh(III), Pd(II) and Au(III)] metal complexes of Schiff bases in alcoholic medium and preliminary in vitro screening for antimicrobial activity showed that the compounds had only moderate antimicrobial activity against S.aureus, Salmonella typhimurium and E. coli with only moderate antibacterial activity.

In present study, a novel Schiff base ligand was synthesized by the reaction of INH with 2-hydroxynicotinaldehyde's (2-hydroxynicotinaldehyde, HTA). This compound is not yet publicly reported nicotinic aldehyde-isonicotinaldehyde (HIN) Schiff base compound, its structural composition was confirmed by FT-IR, XRD, 1H NMR, XPS and in vitro antimicrobial activity against E. coli and S. aureus was determined by liquid and plate assays, and the synthetic route is shown below in Scheme 1.

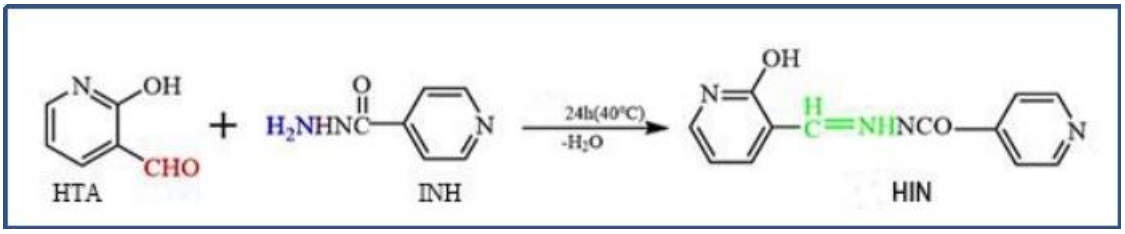

Scheme 1 Schiff base synthesis routine of INH and HTA.

2. Experimental

2.1 Materials

2-Hydroxynicotinaldehyde (AR) and agar powder (AR) were purchased from Shanghai Aladdin Biochemical Science and Technology Co., Ltd; isoniazid (AR) was purchased from Shanghai McLean Biochemical Science and Technology Co., Ltd; peptone (BR) and yeast leaching powder (BR) were purchased from Beijing Auoboxing Biotechnology Co., Ltd; sodium chloride (AR) was purchased from Chengdu Kelon Chemical Co. *E.coli/ S.aureus* strains were preserved in our Lab. Fourier Infrared Spectrometer (NicoLet Is 1); X-ray Single Crystal Diffractometer (XRD-7000S/L); Low Temperature Differential Scanning Calorimeter (DSC 3500 Sirius); Nuclear Magnetic Resonance Popper (Bruker 600M); X-ray Photoelectron Spectroscopy (Thermo SCIENTIFIC ESCALAB Xi); Economical Benchtop Ultrapure Water (WP-RO-20B); Enzyme Labeling Instrument (K6600A); Constant Temperature Incubator (NicoLet Is 10).

2.2 Synthesis of isoniazid/2-hydroxynicotinaldehyde Schiff base

Weigh 0.412g (0.003mol) INH powder, 0.123g (0.001mol) HTA powder dissolved in 30mL of deionized water, stirring dissolved in a water bath at 40℃ for 48h, to be removed from the solution from light yellow to yellow and then stood still at room temperature to slowly evaporate the growth of crystals, to be obtained after the water evaporation of the golden-yellow powder, that is, for the desired Schiff base compound.

2.3 Characterization

(1) Fourier Transform infrared spectroscopy (FT-IR) The samples were prepared by pressing the samples, weighing the samples and potassium bromide according to 1:100 and mixing them in an onyx mortar, grinding them uniformly, and then pressing them into a transparent thin film for testing. The scanning wavelength was 4000~400cm^{-1}, the resolution was 4cm^{-1}, and the number of scans was 32. (2) X-ray Diffraction (XRD) Appropriate amount of sample was taken in the XRD sample slot, flattened with a coverslip, and the scanning rate was set at 5°/min, with a scanning range of 10-60º. (3) Differential Scanning Calorimetry (DSC) Take 5-10mg of sample sealed in a crucible, the sample in the flow rate of 25mL/min nitrogen environment, the scanning temperature range of 100-240°C, scanning rate of 5°/min. (4) Nuclear Magnetic Resonance Hydrogen Spectrometry (1H-Nuclear Magnetic Resonance, ^{1}HNMR) INH, HTA and HIN were dissolved in deuterium water and deuterated methanol, respectively, and were measured using a nuclear magnetic spectrometer at 600 MHZ. (5) X-ray photoelectron (X-ray Photoelectron Spectroscopy, XPS) Take an appropriate amount of dry samples pressed film made of solid film, the area size of 0.5cm × 0.8cm, the thickness of less than 4mm, the scanning voltage of 14795.40V, the target current 50mA.

2.4 Antibacterial activity

Solution method 200μL of freshly prepared *E.coli/ S.aureus* bacterial solution was pipetted into a 96-well plate for dilution until the OD_{600} value was 0.129 (0.129≈10^{8}CFU). 0.0805g of INH, HTA and HIN were dissolved in 100mL of anhydrous ethanol with stirring to dissolve, respectively, and three sets of parallel liquid antimicrobial experiments were carried out in 96-well plates, with the final concentrations of the drugs being 805.00μg/mL, 402.50μg/mL, 201.25μg/mL, 100.63μg/mL, 50.31μg/mL, 25.16μg/mL, 100μL of bacterial solution was added to each well and then placed in a thermostatic incubator (37℃) for 24h, and the OD_{600} value was determined using an enzyme marker.

Solid plate method Freshly prepared *E.coli /S.aureus* bacterial solution was diluted to 10^{8}CFU, 10^{7}CFU, 10^{6}CFU, 10^{5}CFU and 10^{4}CFU, and 100μL of different concentrations of the bacterial solution were smeared and coated on the surface of solid culture medium, sealed with sealing film, and put into a constant temperature incubator (37℃) for 12h, and single dispersed colonies successively grown were selected to conduct subsequent solid antimicrobial experiments. Accurately weigh 0.075g, 0.3g, 0.6g of INH, HTA and HIN were dissolved in 60mL of deionized water, and the final concentrations of the drugs were 1.25mg/mL, 5.00mg/mL and 10.00mg/mL, stirred and dissolved, and then put into the sterilizer to be sterilized for 2 h, and then poured into the plate after sterilization, and then sucked up 100 μL of diluted bacterial solution (*E.coli /S.aureus*) was coated and put into a constant temperature incubator (37℃) for 12h.

2.5 Antimicrobial determination

Isoniazid (INH), 2-hydroxynicotinaldehyde (HTA), isoniazid (INH)/2-hydroxynicotinaldehyde (HIN) solutions at concentrations of (2MIC) and HIN solutions at concentrations of 201.25μg/mL and 100.63μg/mL (null inhibitory concentration) were configured, respectively. Single colonies of *E.coli /S.aureus* were selected and incubated in 2.0 mL of LB medium at 37℃ and 180 rpm until the OD_{600} values of *E.coli and S.aureus* were 0.6 and 1.1, respectively.Taking 2mL of bacterial solution was mixed with 2.0 mL of drug solution with a concentration of 2 MIC (measured in

experiment 2.4) to make the final concentration of the drug 1 MIC and incubated at 37°C/180rpm for 6h. Centrifuge the bacterial solution at 4°C at 3000rpm for 5min, collect the bacterial pellet, disperse in 1.0 mL of PBS and repeat the above steps 3 times to remove organic residues. Sample preparation: 50μL bacterial solution was added dropwise onto a copper mesh, dried naturally for 8-10 h and then characterized by SEM.

3. Results and Discussions

3.1 Characterization

Figure 1a shows the FT-IR spectra of INH, HTA and HIN, from which it can be seen that the infrared absorption peak of ν (N-H) of the amino group of INH disappeared at 3304cm^{-1}. It was initially inferred that the primary amine group of INH was involved in the Schiff base reaction. 1700-1500cm^{-1} were the absorption peaks generated by the vibration of the pyridine ring skeleton of HTA, the w (N-H) on the amide, the w (N-H) of the amine group, the ν (C=O) and w (C-N) produced absorption peaks, and the absorption peaks of the aldehyde group of HTA disappeared at 1750-1665cm^{-1}, which tentatively inferred that the C＝O of HTA was also involved in the Schiff base reaction. Compared to HTA and INH, HIN produced a new expansion vibration peak at 3359cm^{-1}, which is the expansion vibration peak produced by the energy reduction of -OH resonating with two pyridine rings; the absorption peak at 3100-3000cm^{-1} is ν (C-H) on the pyridine ring; the absorption peak of C＝N twisted vibration was detected at 3195cm^{-1}; the absorption peak at 1800-1200cm^{-1} absorption peaks were generated by the C＝N resonance vibration, which is significantly different from that of INH and HTA, and HIN. Two energy bands at 1662cm^{-1} were energy bands formed by the ligand imine group ν(C=N), which is basic ally consistent with the reported results in literature [29]; w(-OH) peaks were appeared at 1100-1000 cm^{-1}, and absorption peaks at 900-600cm^{-1} were formed by the pyridine rings of the w(C-H) and w(N-H) of -NH_2. The FT-IR spectroscopic results indicated that INH reacted with HTA by a Schiff base reaction to produce the new compound HIN. Figure 1a2 shows the XRD patterns of INH, HTA and HIN. INH has characteristic diffraction peaks at 2θ=12.02°, 14.34°, 15.68°, 16.76°, 19.60°, 24.28°, 25.44°, 26.10°, 27.30°, 28.88°, and 32.16°, and HTA has characteristic diffraction peaks at 2θ= 15.02°, 18.36°, 26.74°, 28.36°, and 40.44°, and unlike the two reactants, the product HIN has a new diffraction peak at 2θ = 10.74°, and the rest have diffraction peaks at 2θ = 14.34°, 18.84°, 19.22°, 25.44°, 26.14°, and 27.18° that were similar to those of INH and HTA., while the diffraction peaks of INH at 2θ=14.34°, 15.68°, 16.76°, 19.60° were not found in the product HIN. The diffraction peaks of INH and HTA at 2θ=14.34°, 19.60° overlapped and the peak intensity of HTA at 2θ=14.34° was decreased, but the peak intensity was increased at 2θ= 19.60°, which showed that HIN has different crystallinity with the two raw materials. Figure 1a3 shows the DSC patterns of INH, HTA and HIN, from which it can be seen that the melting peaks of the raw materials INH and HTA are at 172°C and 222°C, and there is a small melting peak of HTA at 218°C, which indicates that there is a shift in the crystalline form of HTA. Unlike the raw material, the melting peak of HIN is at 159°C, but the peak shape is not as sharp as that of the raw material, which indicates that there may be impurities in the product HIN or there may be a transformation of the crystal form.

Figure 1b shows the C1s energy level profiles of INH, HTA and HIN.The main peaks of INH are at 284.80eV, 285.33eV, 287.75eV, the binding energies of C-C and C-H are 284.80eV, the characteristic peaks at 285.33eV, 287.75eV are generated by C-N, C=O, and the 291.65 The satellite peak at eV is the trailing peak produced by pyridine ring π-π conjugation.The main peaks of HTA are at 284.85eV, 285.35eV, 287.50eV, the characteristic peaks produced by C-C, C-O, C=O, respectively, and the trailing peak produced by the HTA pyridine ring π-π conjugation is at 291.45eV.The characteristic peaks of HIN for C-C are at 284.45eV, and the characteristic peaks of C-O, C-N characteristic peaks overlap at 286.00eV, C=O characteristic peak at 287.6eV, a new characteristic peak is generated at 292.6eV is the characteristic peak of the reaction-produced C=N,

the pyridine ring π-π conjugation produces satellite peaks at 295.40eV. The characteristic peaks of the product HIN are all trying to move in high field compared to the raw material, also because there is a bigger HIN molecule within the conjugation system, which disperses the electrons around the carbon, and electron density decreases the peaks move to higher field. Newly generated C=N peaks provide further evidence that the Schiff base reaction has synthesized the new substance HIN.

Figure 1c shows the ^{1}H NMR spectra of INH, HTA and HIN, the hydrogen spectrum of INH has a stronger amide group electron supplying effect, and the aromatic hydrogens located in its two neighboring positions peaked in the higher field, corresponding to the signal peak is δ 7.51(d,2H), and the other two aromatic hydrogens corresponded to δ 8.50(d,2H), due to the reagent used in the test is deuterium reagent is D_2O, and the hydrazide nitrogen on the Since the reagent used in the test is the deuterated reagent is D_2O, the active hydrogen on the hydrazide nitrogen does not show a peak and only the aromatic hydrogen on the pyridine ring shows a peak. In Figure 4(b), the signal peak of the hydrogen of aldehyde group of HTA is δ 9.91(s,2H), which is shifted in the lowest field of the spectrum; the aldehyde group, as a strong electron-absorbing group, and its neighboring aromatic hydrogen peak is in the lower field, which corresponds to δ 8.24(d,1H); the active hydrogen of phenol hydroxyl group does not appear, and the phenol hydroxyl group, as a hydrogen-electron-donating group, and its counterpart aromatic hydrogen peak is in the higher field, which is δ 6.66(t,1H); the active hydrogen of phenol hydroxyl group does not appear; and the aromatic hydrogen of phenol hydroxyl group in the opposite field is in the lower field, which corresponds to δ 6.66(t,1H); and the active hydrogen of the phenol hydroxyl group does not appear, but it is in the lower field. ,1H); the signal peak of the remaining one hydrogen is δ 7.84 (d,1H). In Figure 4(c), the newly generated C=N in HIN is an electron-withdrawing group, which reduces the electron-donating effect of the amide group, and the hydrogens from the INH pyridine ring are all shifted to the lower field, and the corresponding signal peaks for the neighboring hydrogen are δ 7.64(dd,2H) and for the interstitial hydrogen are δ 8.57(dd,2H); the density of the electron cloud of the formation of the pyridine ring and the C=N in π-π conjugation is increased, and the aldehydic group from HTA hydrogen evolved into -CH=N- moved to the lower field, and the signal peak changed from δ 9.91(s,2H) to δ 8.48(s,1H), which was the same as the data reported in the literature [30]; the corresponding signal peaks of the remaining -CH=N- neighboring, interstitial, and para-hydrogens on the pyridine ring of HIN were δ 8.65(d,1H), δ 6.41(t,1H), and δ 7.80(d,1H), respectively.

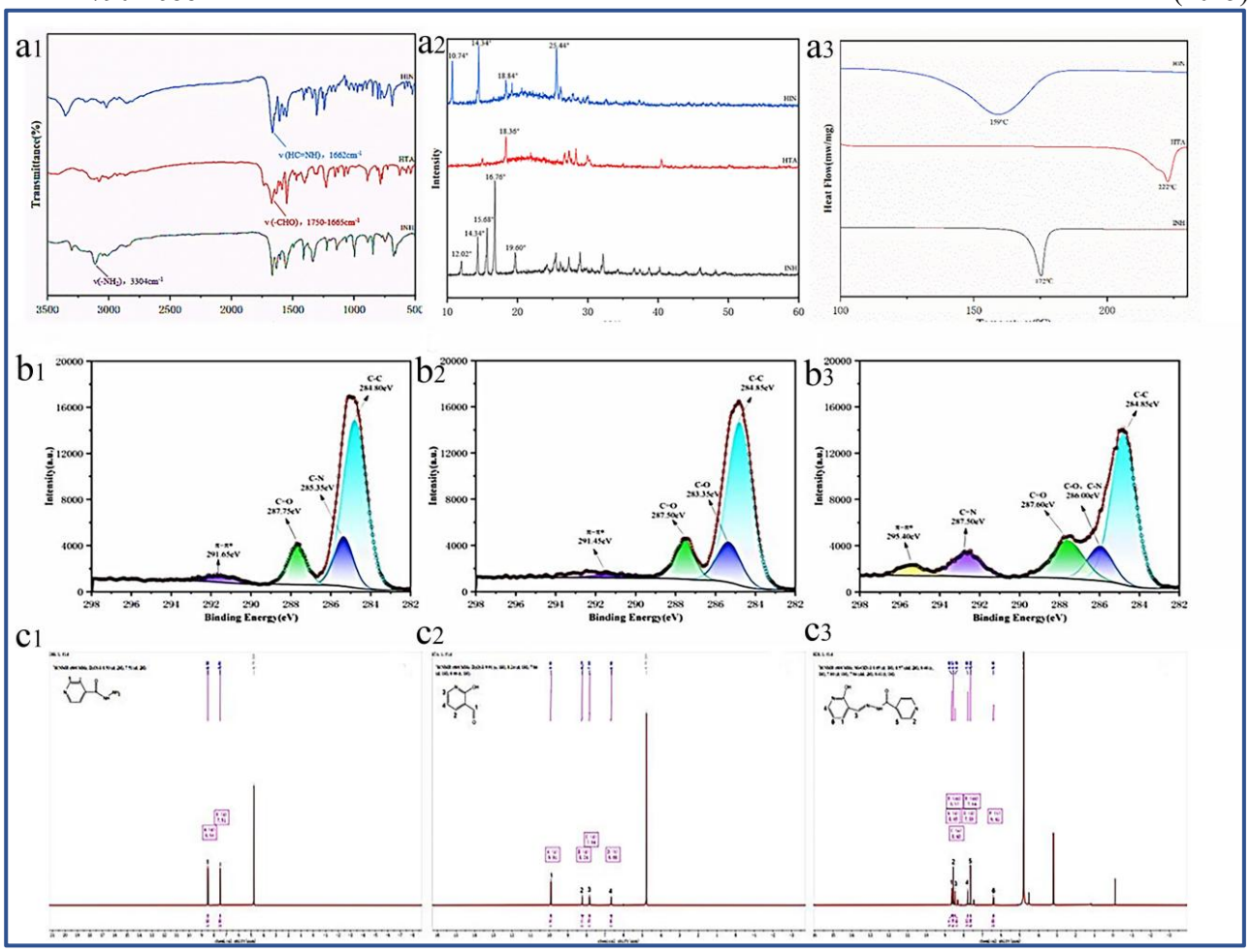

Figure 1 FT-IR(a),XPS(b) and NMR(c) spectrum of INH, HTA and HIN.

3.2 Evaluation of antibacterial activity

From Figure 2a, it can be seen that the blank control (200 μL of pure bacterial solution) parallel experiments showed that INH, HTA, HIN, and ethanol had antibacterial properties against *S.aureus*, and the INH, HTA, and HIN group with ethanol group (solvent) also proved that INH, HTA, and HIN also had some antibacterial properties against *S.aureus*. As the concentration of INH, HTA, HIN and ethanol decreased, the OD_{600} value of *S.aureus* suspension gradually increased with concentration-dependent tolerance, and the OD_{600} value of suspension gradually decreased when the concentration of INH, HTA and HIN was greater than 25.16μg/mL; when the concentration of INH, HTA and HIN was 805.00μg/mL, the bacterial suspension The OD_{600} value was the smallest, and the OD_{600} value of HIN suspension at each concentration was smaller than that of HTA and INH suspension, which indicated that the antimicrobial effect of HIN on *S.aureus* was better than that of HTA and INH. This was also confirmed by Figure 2b, where the bacterial suspension started to clarify when the concentration of HIN was 50.31μg/mL and the suspension was completely clarified at a concentration of 100.63μg/mL; whereas the bacterial suspension only started to clarify when the concentration of INH was 100.63μg/mL and the suspension was completely clarified at a concentration of 201.25μg/mL; the concentrations at which the bacterial suspension was allowed to start clarifying and completely clarifying by HTA were respectively 201.25μg/mL, 402.50μg/mL. As can be seen from Figure 2c: the parallel experiments of blank control (200 μL pure bacterial solution) showed that INH, HTA, HIN, and ethanol had antibacterial properties against E. coli, and the INH, HTA, and HIN groups with ethanol group (solvent) also proved that INH, HTA, and HIN also had some antibacterial properties against E. coli. As the concentration of INH, HTA, HIN and ethanol decreased, the OD_{600} value of *E.coli* suspension gradually increased with concentration-dependent tolerance, and the OD_{600} value of suspension gradually decreased when the

concentration of INH, HTA and HIN was more than 25.16μg/mL; and the OD_{600} value of suspension was minimized when the concentration of INH, HTA and HIN was 805μg/mL, and the OD_{600} value was minimized under most concentration conditions. The OD_{600} value of HIN suspension was smaller than that of HTA and INH under most concentration conditions, which indicated that the antimicrobial effect of HIN on *E.coli* was better than that of HTA and INH. From Figure 2d, it can be seen that the bacterial suspension began to clarify when the concentration of HIN was 50.31μg/mL, and the bacterial suspension was completely clarified when the concentration was 100.63μg/mL; whereas the bacterial suspension only began to clarify when the concentration of INH and HTA was 100.63μg/mL, and the bacterial suspension was completely clarified when the concentration was 201.25μg/mL. Figure 2e shows more intuitively that INH, HTA, and HIN have antimicrobial and concentration-dependent resistance to *S.aureus* and *E.coli*, and the inhibitory effect of INH, HTA, and HIN on *E.coli* was better than that of *S.aureus* at the same concentration. The results showed that INH, HTA, and HIN had antibacterial effects on *E.coli* and *S.aureus* with concentration-dependent tolerance, and HIN had the best antibacterial effect on *E.coli* and *S.aureus*, and the minimum inhibitory concentrations of INH, HTA, and HIN on *S.aureus* were 402.50μg/mL, 402.50μg/mL, respectively, 201.25μg/mL, and the minimum inhibitory concentrations were 402.50μg/mL, 402.50μg/mL, and 100.63μg/mL for *E.coli*, respectively, and the antibacterial effects of INH, HTA, and HIN were more obvious for *E.coli* than for *S.aureus*.

Figure 2f shows the physical drawings of *S.aureus* and *E.coli* concentration gradient diluted to 10^8CFU (a), 10^7CFU (b), 10^6CFU (c), 10^5CFU (d), and 10^4CFU and then coated into the constant temperature incubator (37 ℃) for 12h, *S.aureus* in the concentration of 10^6CFU when the colonies grown dispersed uniformly, and *E.coli* grew at a concentration of 10^5CFU with uniformly dispersed colonies, and subsequent experiments with *S.aureus* and *E.coli* suspensions were taken at concentrations of 10^6CFU(c) and 10^5CFU, respectively. From Figure 2g, it can be seen that compared with the blank group, INH, HTA and HIN have antibacterial effect on *S.aureus*, and the raw material HTA has the best inhibitory effect on *S.aureus*, because no colonies were found in the plates of the three concentration gradients of HTA. The number of colonies in the corresponding plates of INH and HIN decreases with the increase of the concentration, which indicates that the antibacterial effect of INH and HIN has concentration dependence. The antimicrobial effects of INH and HIN were concentration-dependent. At a concentration of 1.25mg/mL, the number of colonies in the plate of INH was significantly larger than that in the plate of HIN, indicating that HIN had a better antimicrobial effect on *S.aureus* at this concentration; when the concentration of INH was not less than 5mg/mL, there were no colonies of *S.aureus* in the plate, while a small number of colonies were still found in the plate of HIN, indicating that the antibacterial effect of INH was better on *S.aureus* at this concentration. antimicrobial effect was better. Figure 2h shows the solid antimicrobial experiments on *E.coli* with different concentrations of HTA, INH and HIN: compared with the blank group, INH, HTA and HIN also have antimicrobial properties on *E.coli*, and the raw material HTA is the most effective on *E.coli* because no colonies were found in the plates of the three concentration gradients of HTA, and the number of colonies in the plates of the three concentration gradients of INH and HIN gradually decreased with the increase of the concentration. INH and HIN showed a gradual decrease in the number of colonies in the corresponding plates with increasing concentration, indicating a concentration-dependent antimicrobial effect. At a concentration of 1.25mg/mL, the number of colonies in the plates of INH and HIN was similar to that of the blank control, indicating that the antibacterial effect of INH and HIN on *E.coli* was not good at this concentration; when the concentration of INH was not less than 5mg/mL, there were no colonies of *E.coli* found in the plates, whereas there were still a large number of colonies in the plates of HIN, indicating that INH had a good antimicrobial effect on *E.coli* at this condition. The results showed that INH and HIN were effective against *E.coli* under these conditions. The results showed that INH, HTA and HIN had antimicrobial properties against *S.aureus* and *E.coli* and HTA had the best antimicrobial effect; when the concentration was

1.25mg/mL, the antimicrobial effect of INH was inferior to that of HIN; when the concentration was not less than 5mg/mL, INH had an excellent antimicrobial effect, and the worst antimicrobial effect was found in HIN. The results of plate assay and liquid assay are different because of the effect of solvent type, the solvent of liquid assay is ethanol and the solvent of plate assay is water, HIN is insoluble in water, and the solubility in ethanol is higher, so the antimicrobial effect is great.

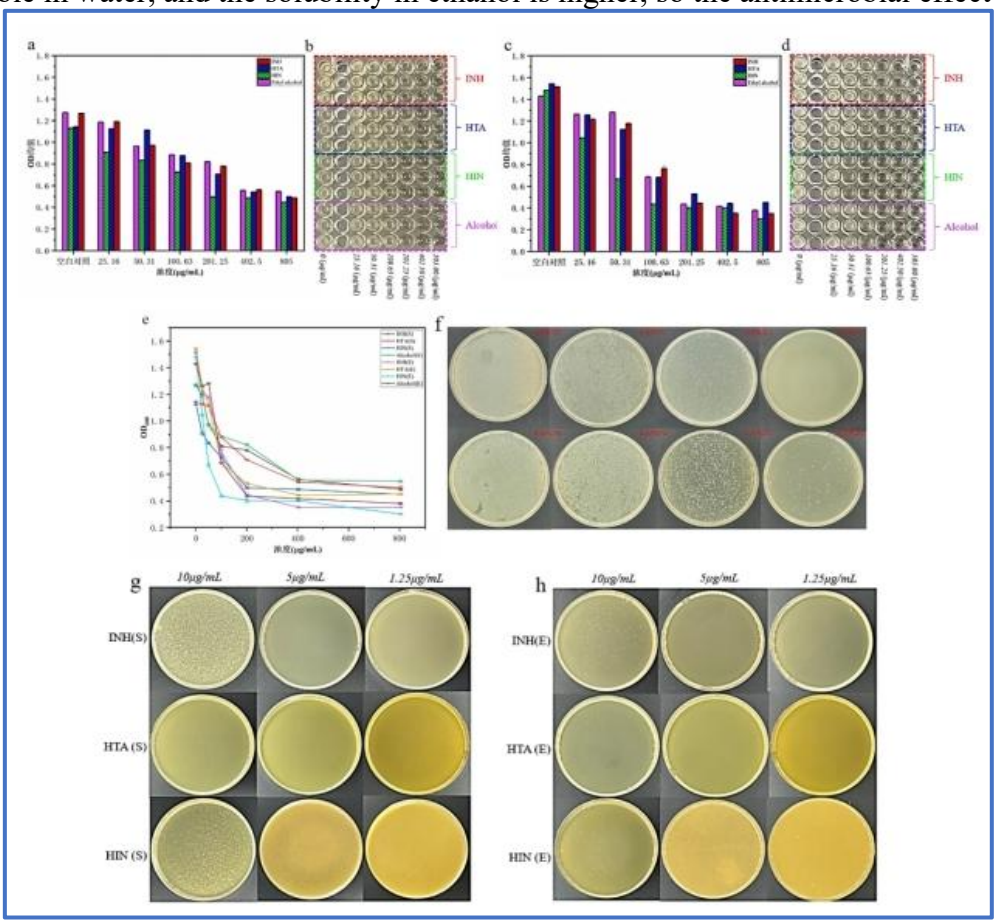

Figure 2 Antimicrobial tests of INH, HTA, HIN against *S.aureus* and *E.coli*. a:Histogram of the me an OD^{600} of *S.aureus* after 24h of INH, HTA, HIN and ethanol (solvent). b:*S.aureus* was incubated with INH, HTA, HIN and ethanol for 24h. c:Mean OD_{600} histogram of *E.coli* after 24h of incubati on with INH, HTA, HIN and ethanol. d:*E.coli* was incubated with INH, HTA, HIN and ethanol for 24h. e:Antimicrobial curves of different concentrations of INH, HTA, HIN and ethanol against *S.au reus* and *E.coli*. f:*S.aureus* and *E.coli* concentrations were diluted to 10^8CFU, 10^7CFU, 10^6CFU, 10^5 CFU and 10^4CFU and then coated at constant temperature for 12h. g:*S.aureus* solid antibacterial exp eriments with different concentrations of HTA, INH and HIN. h:Actual antibacterial experiments of *E.coli* with different concentrations of HTA, INH and HIN.

3.3 SEM observation

Figure 3 shows the SEM images of *S.aureus* and *E.coli* after incubation in INH, HTA, and HIN solutions for 6 h. From Figures 3a and 3f, it can be seen that the bacterial morphology of *S.aureus and E.coli* without the addition of the drugs was full, and the cell walls were smooth without any depression, wrinkles, and rupture, and the normal intact globular and rod-like structures were visible. However, *S.aureus* after treatment with all three compounds showed depressions, and obvious changes in cell morphology could be observed, the cell membrane appeared wrinkled and showed deflated state, and at the minimum inhibitory concentration, the three compounds had similar inhibitory effects on *S.aureus*, but the minimum inhibitory concentration of INH and HTA was twice as much as that of HIN. Figure 3d (minimum inhibitory concentration) and Figure 3e (ineffective inhibitory concentration) showed that HIN at minimum inhibitory concentration made

the cell membrane of *S.aureus* wrinkled more obviously and the number of wrinkled cells was more. The smaller size of *E.coli* and the depression on the cell surface after INH treatment (Figure 3g) indicated that the INH antimicrobial mechanism was to inhibit the growth of bacteria and disrupt the cell membrane. Figure 3h shows that HTA kills the bacteria by directly disrupting the cell membrane and loss of intramembrane material resulting in the deflated state of the cell. The product HIN also achieves the bactericidal effect by crumpling the cell membrane. From Figure 3i (minimum inhibitory concentration) and Figure 3j (ineffective inhibitory concentration), it can be seen that as the concentration of HIN decreases, the degree of crumpling of the cell membrane decreases, and the product's antimicrobial effect on *E.coli* is better than that of *S.aureus*.

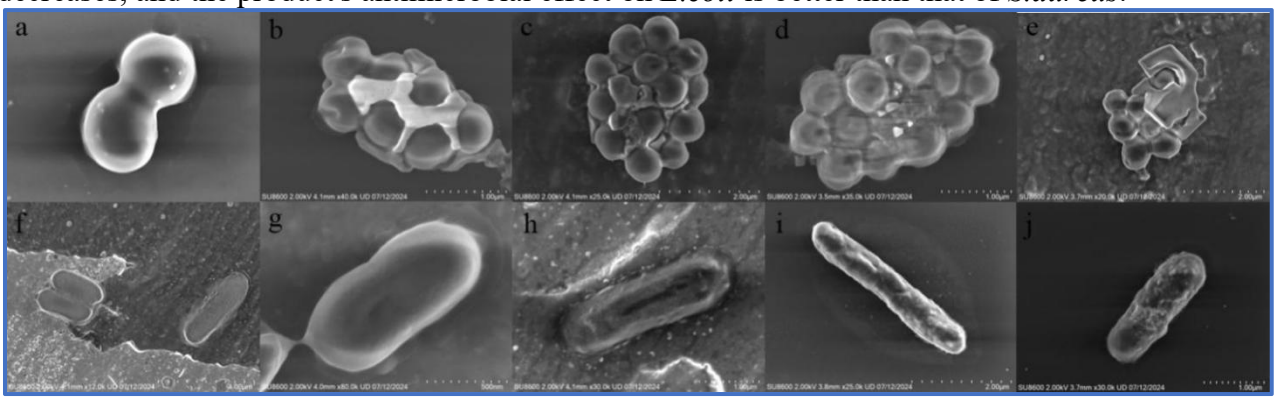

Figure 3 SEM images of *S.aureus*(a-e) and *E.coli*(f-j) after 6h of incubation in INH, HTA, HIN sol ution. a: Negative control of *S.aureus*; b:INH 402.50μg/mL(*S.aureus*); c:HTA 402.50μg/mL(*S.aureus*); d:HIN 201.25μg/mL(*S.aureus*), e:HIN 100.63μg/mL(*S.aureus*); F: Negative control of *E.coli*; g:INH 402.50μg/mL(*E.coli*); h:HTA 402.50μg/mL(*E.coli*); i:HIN 100.63μg/mL(*E.coli*), j:HIN 50.31μg/mL(*E.c oli*).

4. Summary

This study synthesized isoniazid/2-hydroxy nicotinoid Schiff base compounds using isoniazid and 2-hydroxy nicotinoid compounds as raw materials in a 40℃ water bath and further evaluated their antibacterial properties. The structure of isoniazid/2-hydroxynicotinal Schiff base compound was confirmed by FT-IR, ^{1}H NMR, DSC, XRD, XPS. Minimum inhibitory concentration against *S.aureus* and *E.coli* was determined by liquid method and plate method. The results showed that the new infrared absorption peak of isoniazid/2-hydroxynicotinal Schiff base compound at 1662cm^{-1} was formed by ligand imine group ν(C=N), and the melting peak decreased to 159℃. There was also a new diffraction peak at 2θ=10.74° on XRD spectra and chemical shift signal peak on the nuclear magnetic hydrogen spectrum. The characteristic peaks of XPS shifted towards higher fields. Minimum inhibitory concentrations of isoniazid, 2-hydroxynicotinoid, and isoniazid/2-hydroxynicotinoid mat compounds against *S.aureus* and *E.coli* were 402.50μg/mL, 402.50μg/mL, 201.25μg/mL, and 402.50μg/mL, 402.50μg/mL, and 100.63μg /mL, respectively.The antimicrobial mechanism of all three drugs kills the bacteria by destroying the cell membrane, and the antimicrobial effect on *E.coli* is better, and the degree of folds of the cell membrane further confirms that HIN has a better antimicrobial effect.

Acknowledgement

Thanks to Science and technology training program of CQUST(202311551010,202411551008).

References

[1] Theuretzbacher U, Bush K, Harbarth S, et al. Critical analysis of antibacterial agents in clinical development[J]. Nature Reviews Microbiology, 2020, 18(5): 286–298.
[2] Cornforth D M, Foster K R. Competition sensing: the social side of bacterial stress responses[J]. Nature Reviews Microbiology, 2013, 11(4): 285–293.

[3] El Tekle G, Garrett W S. Bacteria in cancer initiation, promotion and progression[J]. Nature Reviews Cancer, 2023, 23(9): 600–618.
[4] Wei S, Chen T, Hou H, et al. Recent advances in electrochemical sterilization[J]. Journal of Electroanalytical Chemistry, 2023, 937(10): 117419.
[5] Linqing M, Shuang Z, Yaping L, et al. Mei L. An overview of the use of nanozymes in antibacterial applications[J]. Chemical Engineering Journal, 2021, 418(16): 129431.
[6] Yuan R, Yan Z, Shaga A, et al. Design and fabrication of an electrochemical sensing platform based on a porous organic polymer for ultrasensitive ampicillin detection[J]. Sensors and Actuators B: Chemical, 2021, 327(2): 128949.
[7] Hrioua A, Loudiki A, Farahi A, et al. Complexation of amoxicillin by transition metals: Physico-chemical and antibacterial activity evaluation[J]. Bioelectrochemistry, 2021, 142(6): 107936.
[8] Niu X, Sun L, Zhang X, et al. Fabrication and antibacterial properties of cefuroxime-loaded TiO2 nanotubes[J]. Applied Microbiology and Biotechnology, 2020, 104(7): 2947–2955.
[9] Wu Z-C, Boger D L. Maxamycins: Durable Antibiotics Derived by Rational Redesign of Vancomycin[J]. Accounts of Chemical Research, 2020, 53(11): 2587–2599.
[10] Bassett B, Subramaniyam S, Fan Y, et al. Minocycline alleviates depression-like symptoms by rescuing decrease in neurogenesis in dorsal hippocampus via blocking microglia activation/phagocytosis[J]. Brain, Behavior, and Immunity, 2021, 91(1): 519–530.
[11] Shabatina T I, Vernaya O I, Melnikov M Y. Hybrid Nanosystems of Antibiotics with Metal Nanoparticles—Novel Antibacterial Agents[J]. Molecules, 2023, 28(4): 1603.
[12] Bin L, Wei W, Dingyuan Y, et al. Multifunctional AIE nanosphere-based "Nananobomba" for tr imodal imaging-guided photothermalphotodynamicpharmacological therapy of drug-resistant bacterial[J]. ACS NANO, 2023, 17(4): 4601-4618.
[13] Gray D A, Wenzel M. Multitarget Approaches against Multiresistant Superbugs[J]. ACS Infectious Diseases, 2020, 6(6): 1346–1365.
[14] Dean A S, Zignol M, Cabibbe A M, et al. Prevalence and genetic profiles of isoniazid resistance in tuberculosis patients: A multicountry analysis of cross-sectional data[J]. PLOS Medicine, 2020, 17(1): 1003008.
[15] Dooley K E, Miyahara S, Von Groote-Bidlingmaier F, et al. Early Bactericidal Activity of Different Isoniazid Doses for Drug-Resistant Tuberculosis (INHindsight): A Randomized, Open-Label Clinical Trial[J]. American Journal of Respiratory and Critical Care Medicine, 2020, 201(11): 1416–1424.
[16] Hu Y-Q, Zhang S, Zhao F, et al. Isoniazid derivatives and their anti-tubercular activity[J]. European Journal of Medicinal Chemistry, 2017, 133(9): 255–267.
[17] Ali B, Mohammed Khan K, Arshia, et al. Synthetic nicotinic/isonicotinic thiosemicarbazides: In vitro urease inhibitory activities and molecular docking studies[J]. Bioorganic Chemistry, 2018, 79(4): 34–45.
[18] Butler M I, Sandhu K, Cryan J F, et al. From isoniazid to psychobiotics: the gut microbiome as a new antidepressant target[J]. British Journal of Hospital Medicine, 2019, 80(3): 139–145.
[19] Feng Y, Guo N, Sun Q, et al. Open-label study of combination therapy with isoniazid for management of refractory neuropathic pain[J]. Journal of Clinical Neuroscience, 2012, 19(8): 1130–1133.
[20] Jeyaraman P, Alagarraj A, Natarajan R. In silico and in vitro studies of transition metal complexes derived from curcumin–isoniazid Schiff base[J]. Journal of Biomolecular Structure and Dynamics, 2020, 38(2): 488–499.
[21] Jia Y, Li J. Molecular Assembly of Schiff Base Interactions: Construction and Application[J]. Chemical Reviews, 2015, 115(3): 1597–1621.
[22] Wen W, Zhang Z, Jing L, et al. Synthesis of a Hein–Schiff base compound and its antibacterial activity on cotton fabrics[J]. Cellulose, 2020, 27(12): 7243–7254.
[23] Mohan B, Choudhary M. Synthesis, crystal structure, computational study and anti-virus effect of mixed ligand copper (II) complex with ONS donor Schiff base and 1, 10-phenanthroline[J]. Journal of Molecular Structure, 2021, 1246(24): 131246.
[24] Hameed A, al-Rashida M, Uroos M, et al. Schiff bases in medicinal chemistry: a patent review (2010-2015)[J]. Expert Opinion on Therapeutic Patents, 2017, 27(1): 63–79.
[25] Uddin M N, Ahmed S S, Alam S M R. Review: Biomedical applications of Schiff base metal complexes[J]. Journal of Coordination Chemistry, 2020, 73(23): 3109–3149.
[26] Yasser M, Abdel B, Ahmed M, et al. Developing a new multi-featured chitosan-quinoline Schiff base with potent antibacterial, antioxidant, and antidiabetic activities: design and molecular modeling simulation[J]. Nature, 2023, 13(1):22792.

[27] Bayeh Y, Mohammed F, Gebrezgiabher M, et al. Synthesis, characterization and antibacterial activities of polydentate Schiff bases, based on salicylaldehyde[J]. Advances in Biological Chemistry, 2020, 10(05):127-139.
[28] Yousif E, Majeed A, Khulood S, et al. Metal complexes of Schiff base: preparation, characterization and antibacterial activity[J]. Arabian Journal of Chemistry, 2017, 2(10):S1639-S1644.
[29] Ahmed M, Abdelazeem S, Esmail M, et al. Novel Cytocompatible Chitosan Schiff Base Derivat ive as a Potent Antibacterial, Antidiabetic, and Anticancer Agent[J]. Arabian Journal for Science and Engineering, 2023, 13(48):7587-7601.
[30] Malhotra M, Sharma S, Deep A. Synthesis, characterization and antimicrobial evaluation of nov el derivatives of isoniazid[J]. Medicinal Chemistry Research, 2012, 21(7): 1237-1244.